Inelastic pp cross-section at 13 TeV

Miguel Arratia
Cavendish Laboratory, University of Cambridge

HEP Seminars, University College London

ISR @ CERN The first hadron collider

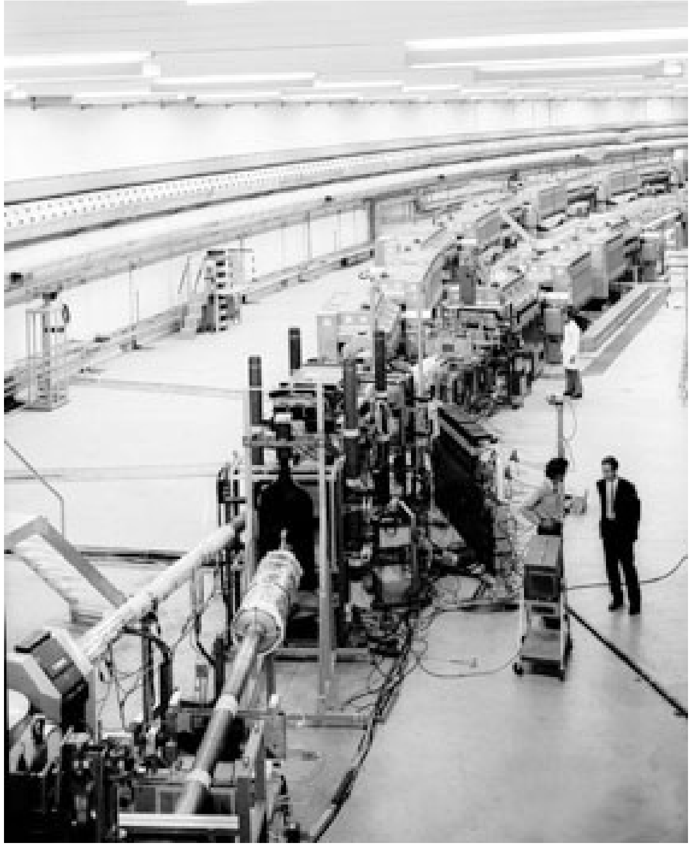

Fig from [1]

- Started operations in 1971
- 300 m diameter
- pp collisions, 62 GeV max.
- Opened new energy regime, x5 times more energy than before

MEASUREMENT OF THE TOTAL PROTON-PROTON CROSS-SECTION AT THE ISR ☆

S.R. AMENDOLIA, G. BELLETTINI*, P.L. BRACCINI, C. BRADASCHIA, R. CASTALDI**, V. CAVASINNI, C. CERRI*, T. Del PRETE, L. FOA*, P. GIROMINI, P. LAURELLI, A. MENZIONE, L. RISTORI, G. SANGUINETTI, M. VALDATA,

Istituto Nazionale di Fisica Nucleare, Sezione di Pisa
Istituto di Fisica dell'Università, Pisa
Scuola Normale Superiore, Pisa, Italy

G. FINOCCHIARO, P. GRANNIS*, D. GREEN, R. MUSTARD and R. THUN

State University of New York, Stony Brook, New York, USA

Received 23 February 1973

We present the first results of a measurement of the total cross-section σ_T in proton-proton collisions at equivalent laboratory momenta between 291 and 1480 GeV/c at the CERN Intersecting Storage Rings (ISR). The method is based on the measurement of the ratio of the total interaction rate and the machine luminosity. The data show an increase of about 10% in σ_T in this energy interval.

Discovery! the cross-section rises with energy

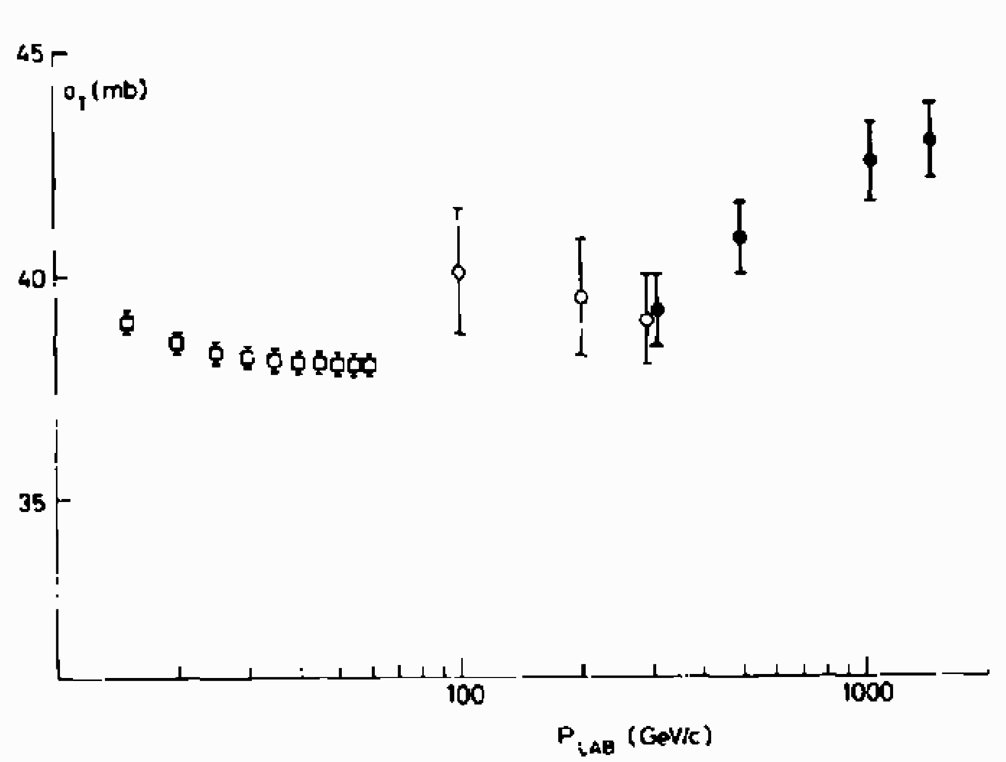

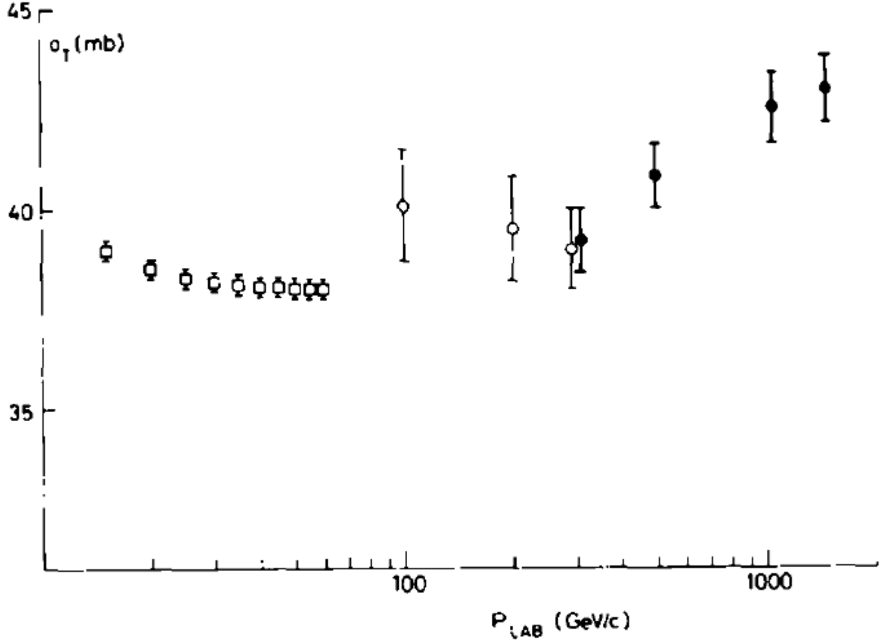

The possibility of rapidly rising total cross-sections at very high energies has been considered theoretically by Heisenberg [10], and by Cheng and Wu [11]. The presence of an energy dependence in σ_T indicates that if an asymptotic limit exists, it has not been reached at ISR energies, and points up the interest in extending all total cross-section measurements to higher energies.

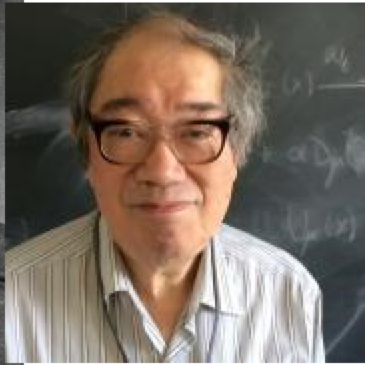

Over 40 years later and still…

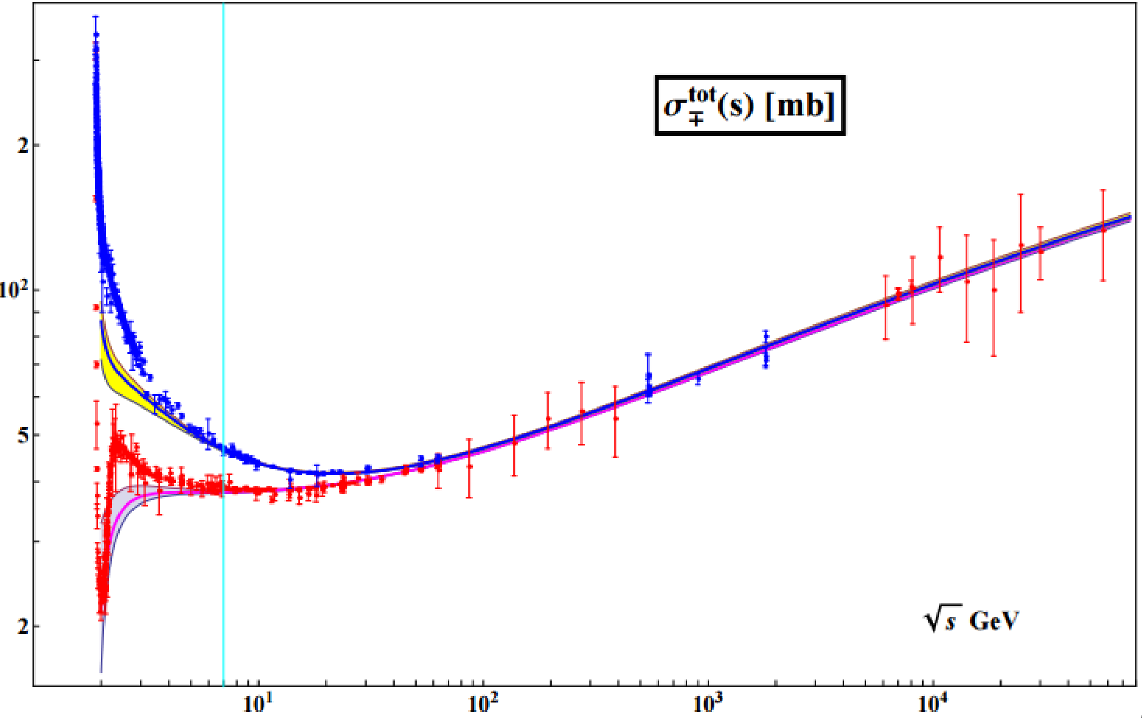

Fig from [2]

Data consistent with:

- 1953: Heisenberg's $\ln^2(s)$ dependence (also with power-law)
- 1961: Froissart bound. i.e cross-section cannot grow faster than $\ln^2(s)$

Cosmic ray data

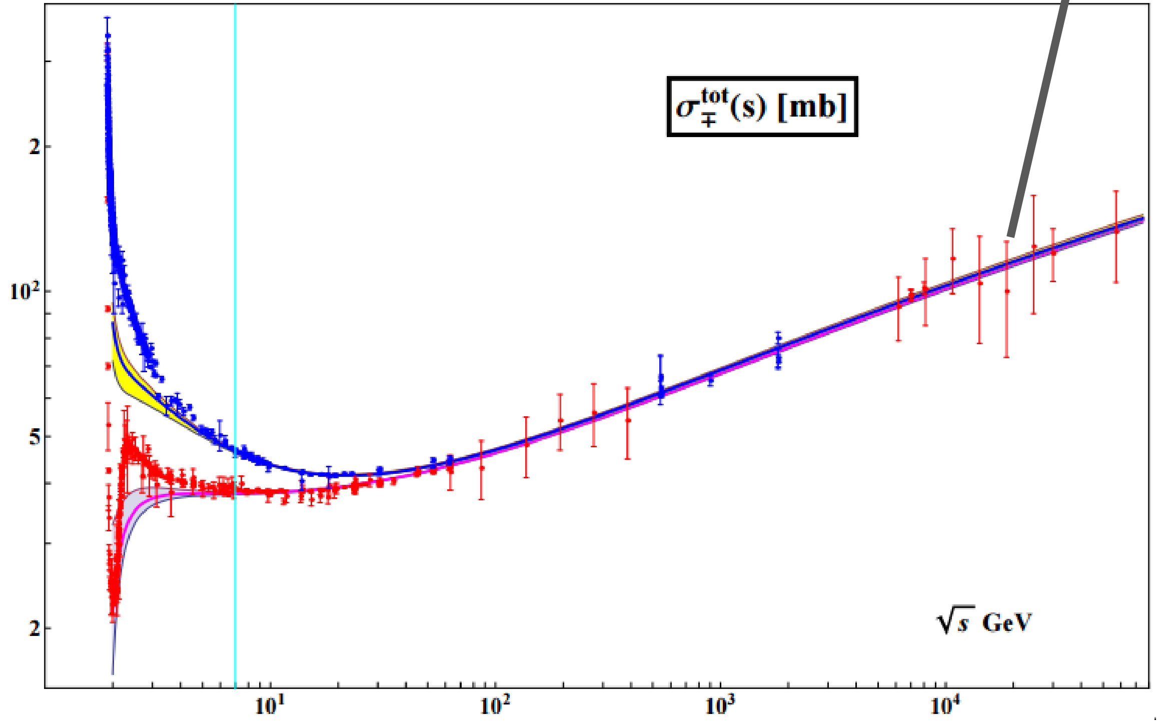

Fig from [2]

- LHC is the first collider to reach up to cosmic ray measurements of cross-sections

Cosmic ray energy spectrum

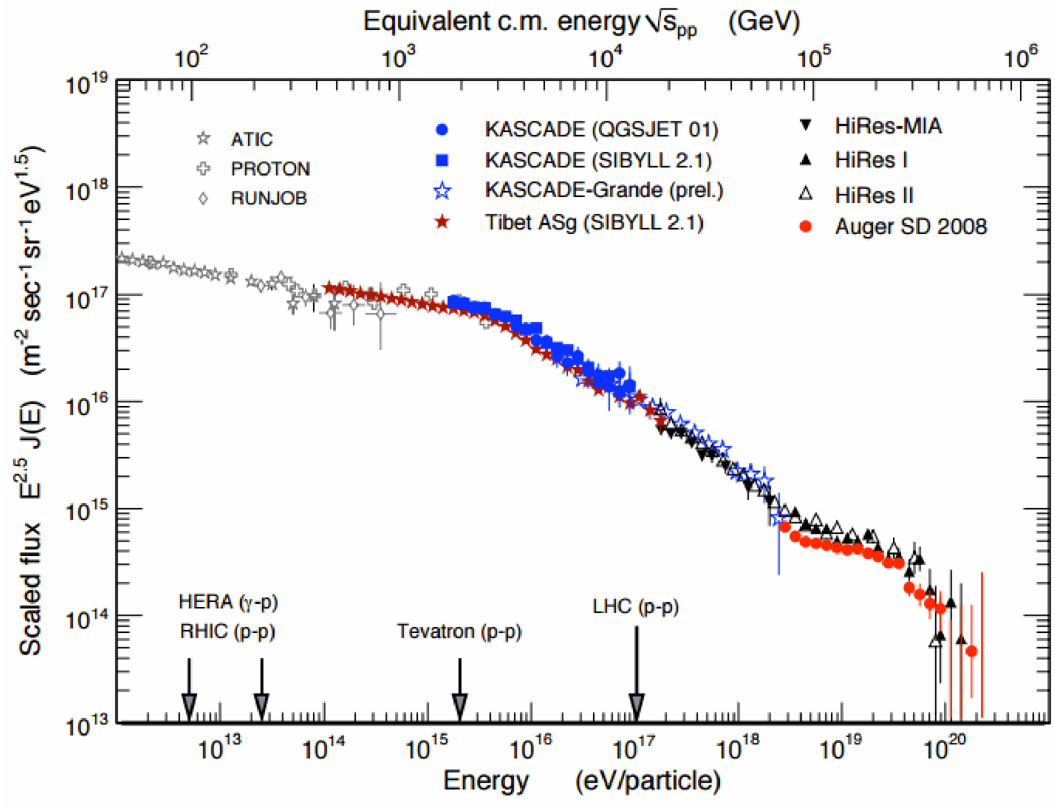

Fig from [3]

- The origin of the “knee” is one of the key open questions in cosmic ray physics
- Composition measurements are required to understand origin

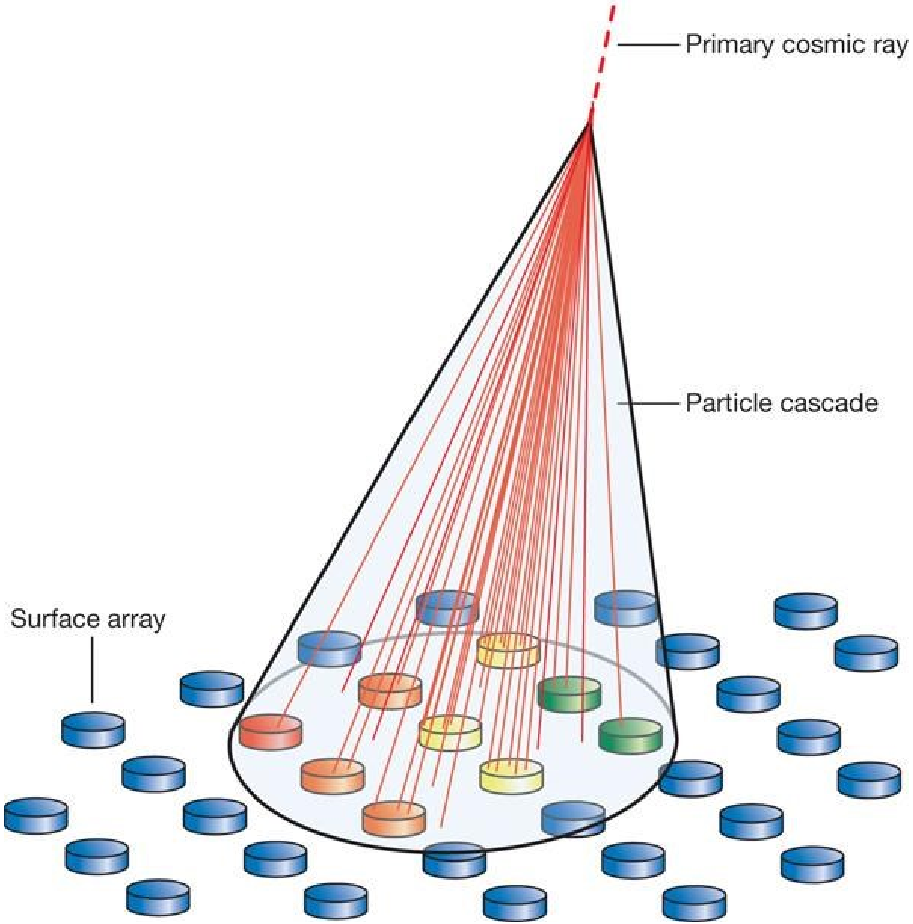

Fig from [4]

- Use the atmosphere as a calorimeter!
- This method does not allow a direct identification of the primary cosmic ray

Shower depth, the main tool for cosmic ray ID

- Inelastic cross-section determines the mean-free-path in the atmosphere

- 13 TeV data is right in the middle of interesting region

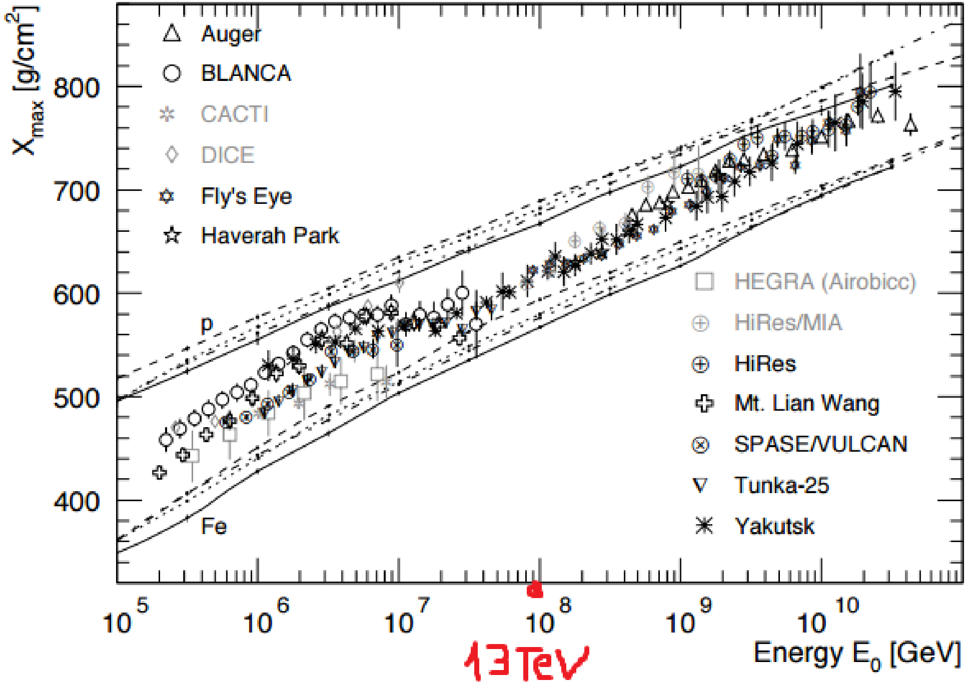

Fig from [5]

LHC energy range overlaps with cosmic ray data

- Data can be used to constrain model that translates p-p to p-air cross-sections

- This model is the backbone of air-shower simulations. It is also used in heavy ion physics

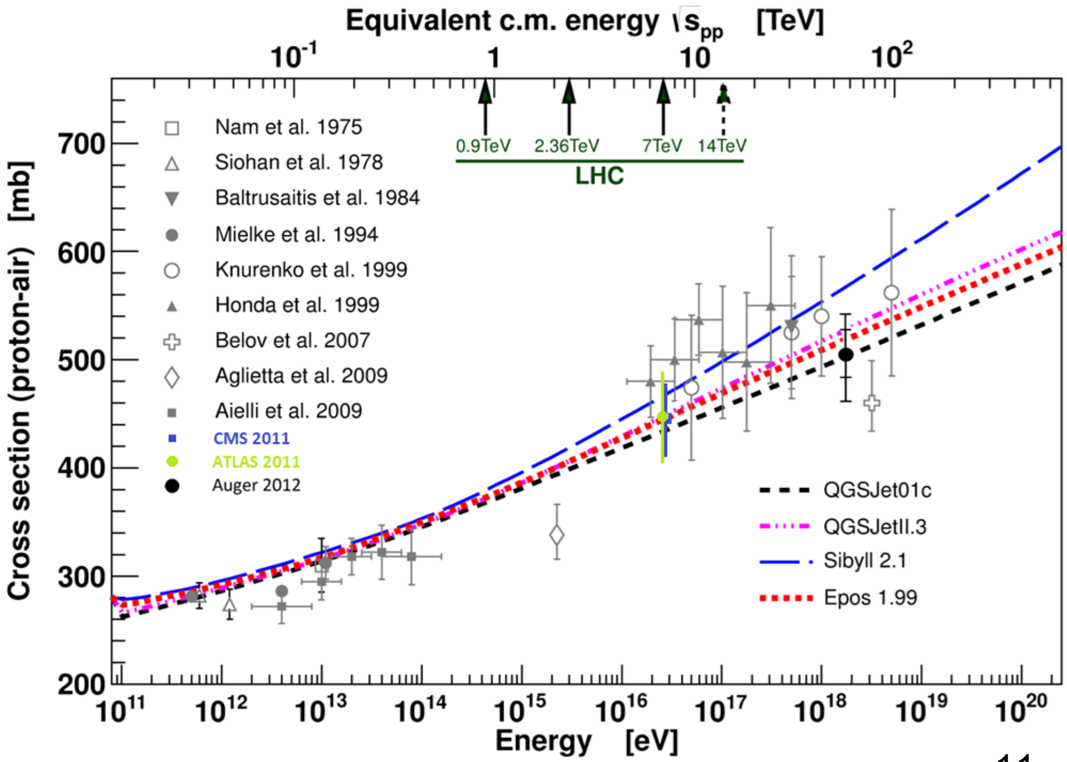

Fig from [6]

Minimum-bias trigger scintillators

- Highly efficient plastic scintillators (24 modules). Completely rebuilt for Run-II

- We trigger on events with at least 1 hit

- Acceptance covers from 14.4 to 2.4 degrees. 15 cm from beam-pipe.

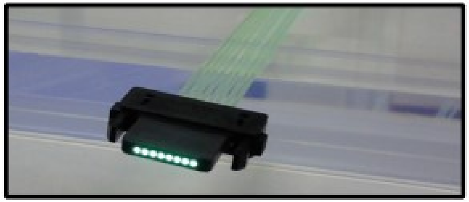

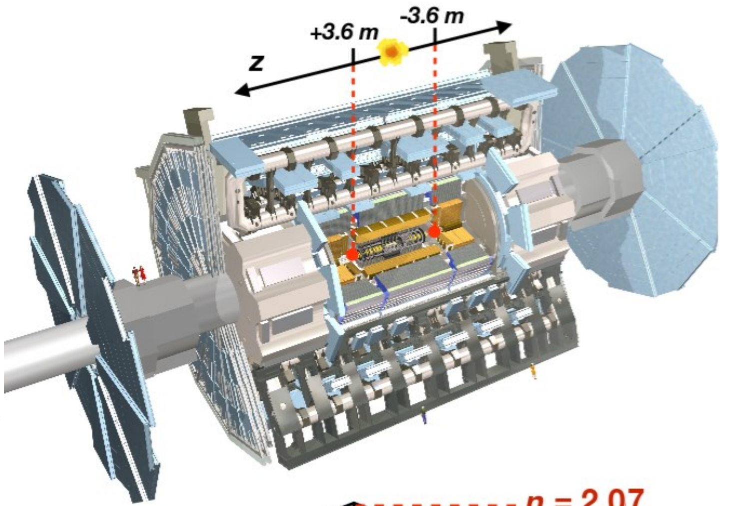

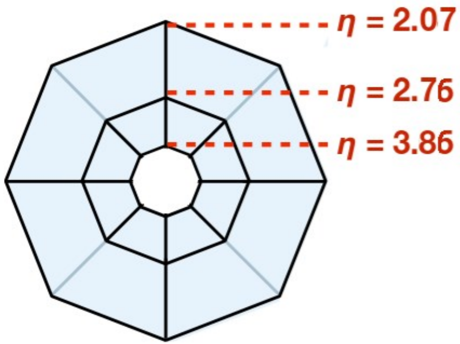

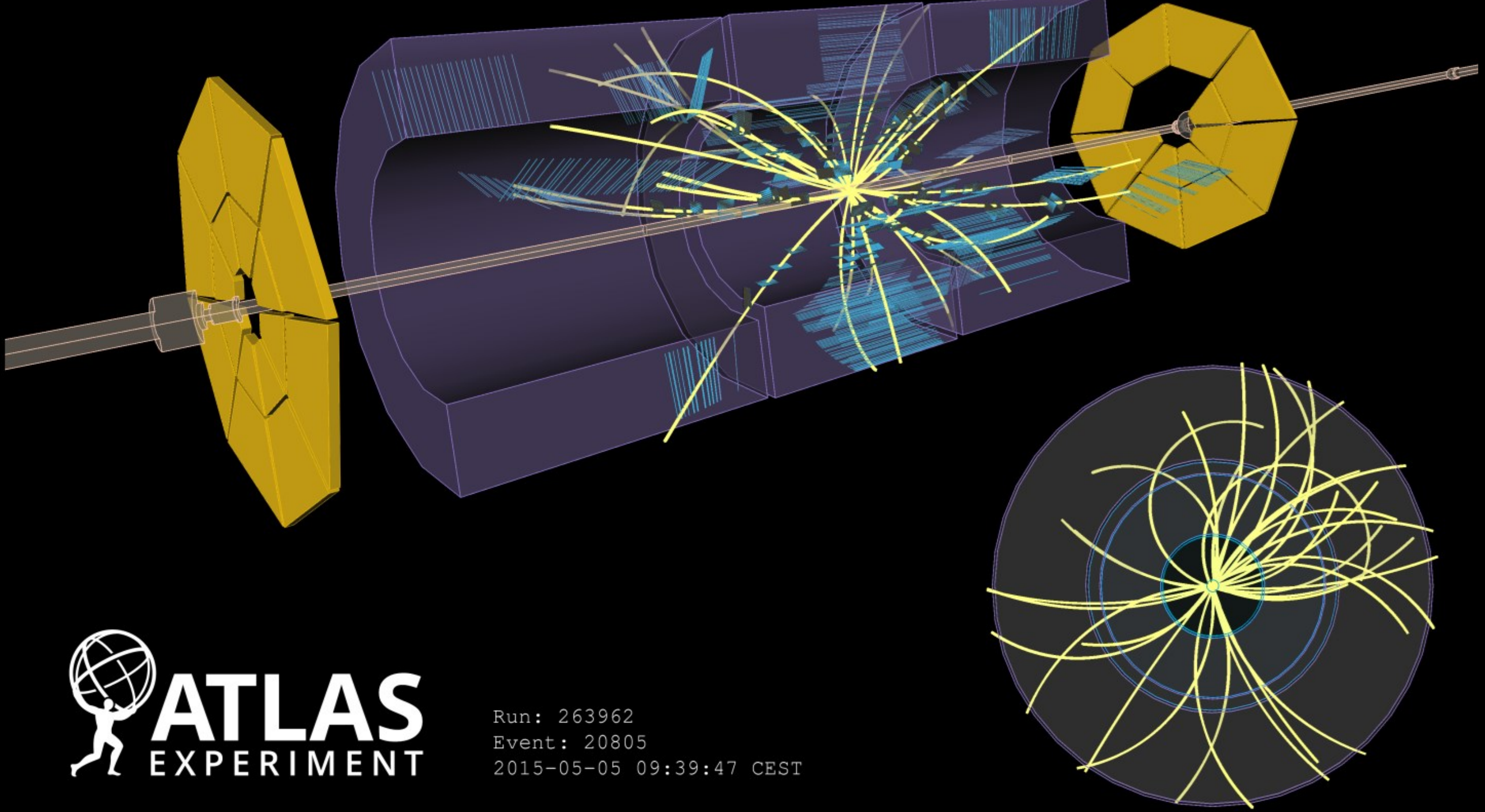
ATLAS
EXPERIMENT
Run: 263962
Event: 20805
2015-05-05 09:39:47 CEST

Special low-luminosity run, July 2015

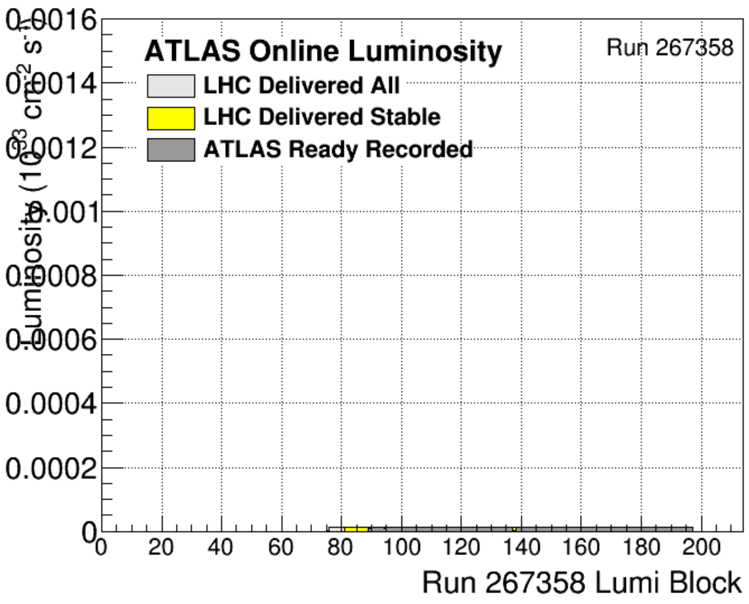

We need negligible "pileup" for this measurement

$\mu \approx 0.002$

About 5M "minimum-bias" events

Breakdown of the inelastic cross-section

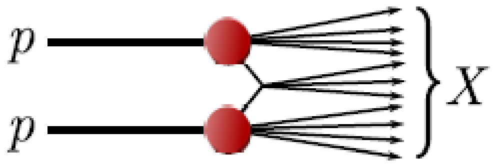

Non-diffractive

~ 70%

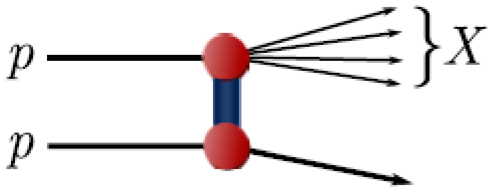

Single-diffractive

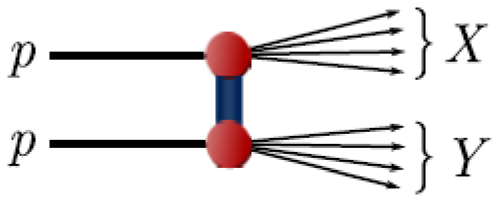

Double-diffractive

~ 30%

Acceptance for low-mass diffractive events

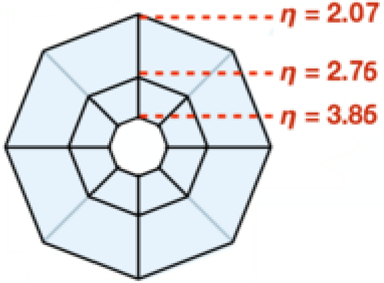

- MBTS has very large acceptance for non-diffractive events

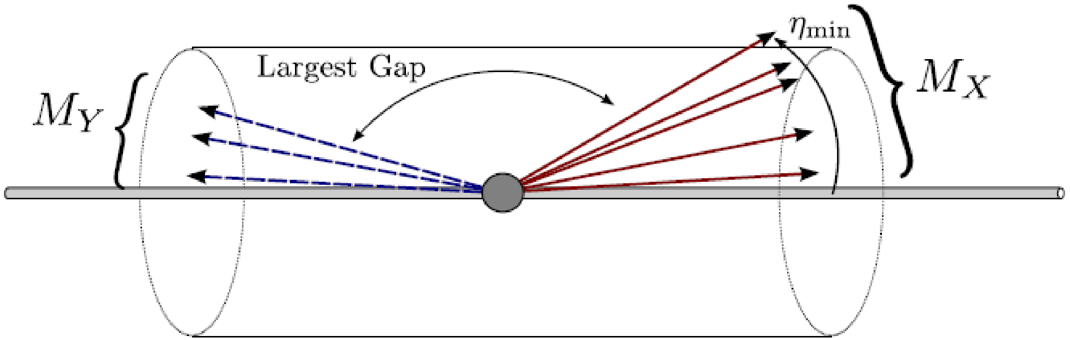

- But, no acceptance for low-mass diffractive events

- Motivates a fiducial region definition

$$\mathcal{A}(M_X) > 50\% \text{ for } M_X > 13 \text{ GeV or}$$
$$\tilde{\xi} \equiv M_X^2/s > 10^{-6}$$

ξ distribution

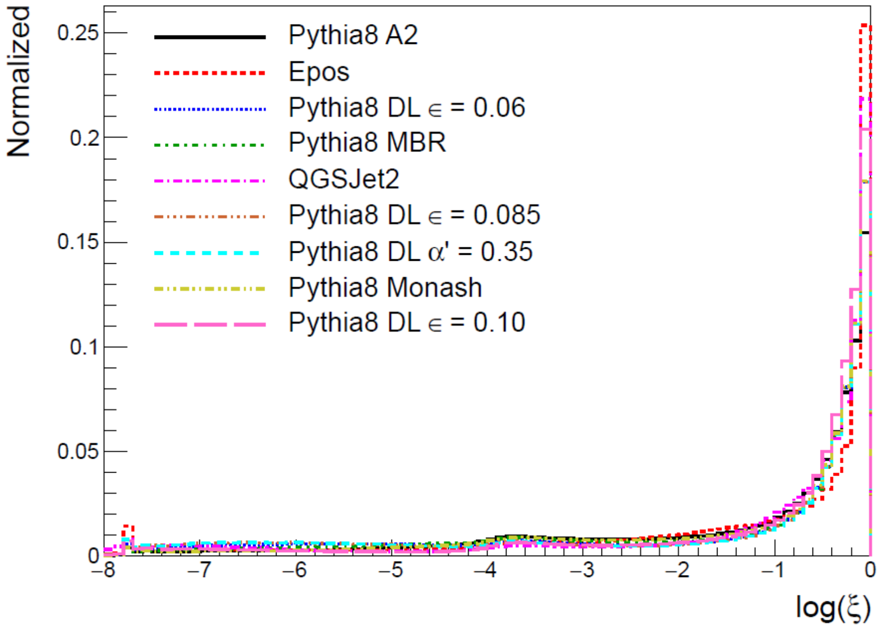

Selection efficiency (2 hits)

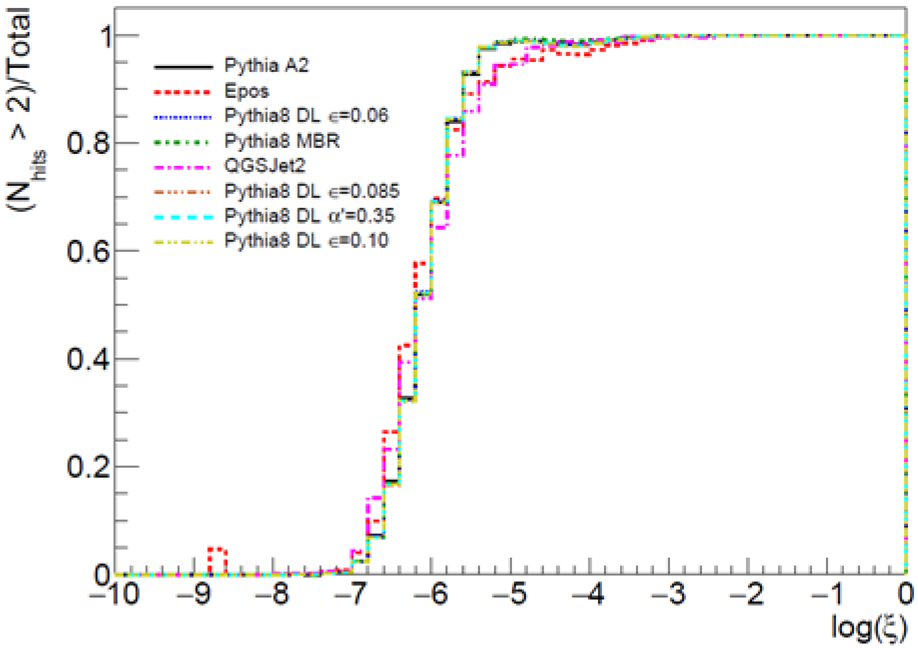

Fiducial cross-section

$$\sigma(\tilde{\xi} > 10^{-6}) = \frac{(N - N_{\mathrm{BG}})}{\epsilon_{\mathrm{trig}} \times \mathcal{L}} \times \frac{1 - f_{\tilde{\xi}<10^{-6}}}{\epsilon_{\mathrm{sel}}}$$

Fiducial region definition chosen to make $C_{MC} \equiv \frac{1-f_{\tilde{\xi}<10^{-6}}}{\epsilon_{\mathrm{sel}}} \approx 1$

ϵ_{sel} = offline selection efficiency for events with $\tilde{\xi} > 10^{-6}$

$f_{\tilde{\xi}<10^{-6}}$ = Migration from outside fiducial region

MBTS efficiency with tracks

$$\epsilon = \frac{\text{Number of counters above threshold and tagged with a track}}{\text{Total number of counters tagged by a track}}$$

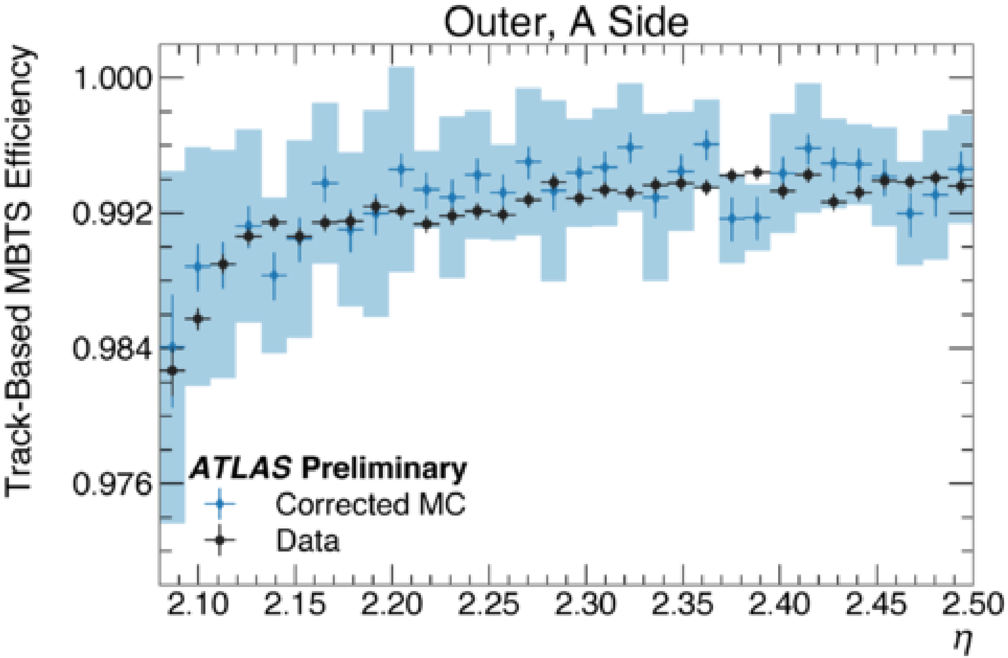

Trigger efficiency

- Measured in data with events selected by other, independent triggers

- Overall 99.7% efficiency

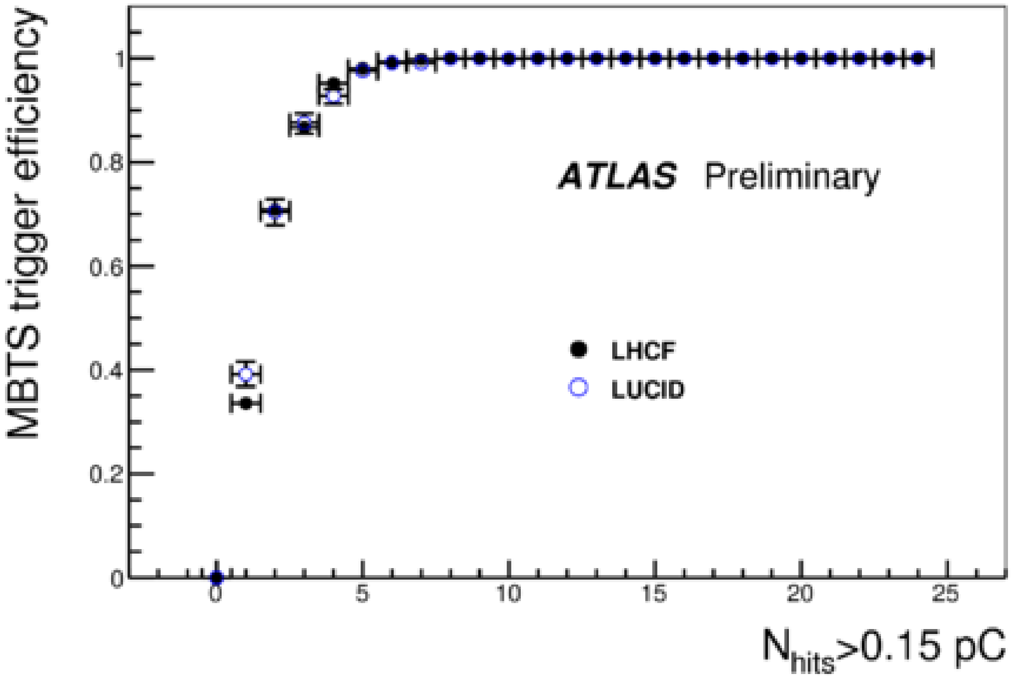

Background

Main sources are:

- Beam-gas interactions
- “Afterglow”, i.e photons & neutrons from nuclear de excitation

We estimate them using dedicated triggers, and timing studies:

0.5% beam-gas and 0.7% afterglow

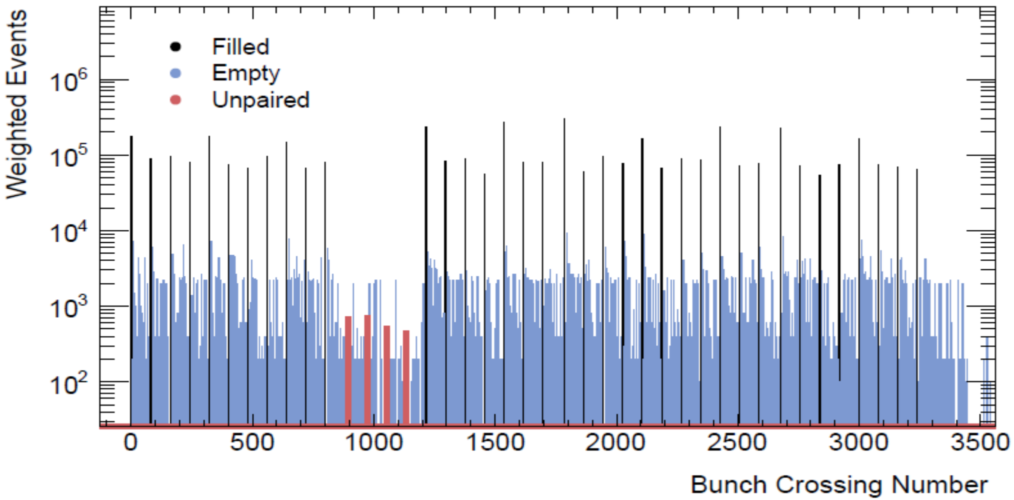

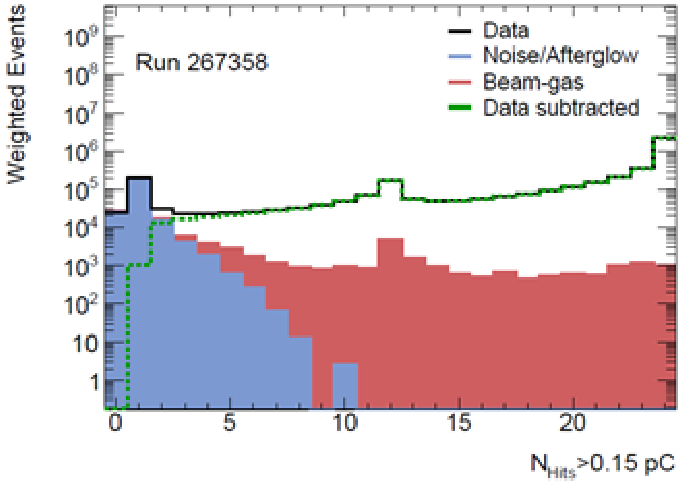

Instantaneous luminosity in a collider

$$\mathcal{L}_{\text{bunch}} = f \times \underbrace{n_1 n_2}_{\text{Bunch current product}} \times \underbrace{\int \rho_1(x,y)\rho_2(x,y)\,dxdy}_{\text{Beam overlap Integral}}$$

f = revolution frequency (27 km / c)

n_1, n_2 = number of protons in bunches

ρ_1, ρ_2 = normalized charge density

$$\mathcal{L} = \sum_{\text{bunches}} \mathcal{L}_{\text{bunch}} \ [\text{cm}^{-2}\text{s}^{-1}]$$

The *van der Meer* method

$$\text{Rate}(\Delta) = c\int \rho_1(x)\rho_2(x-\Delta)dx$$

$$\int \text{Rate}(\Delta)d\Delta = c\int \rho_1(x)\int \rho_2(x-\Delta)d\Delta dx$$

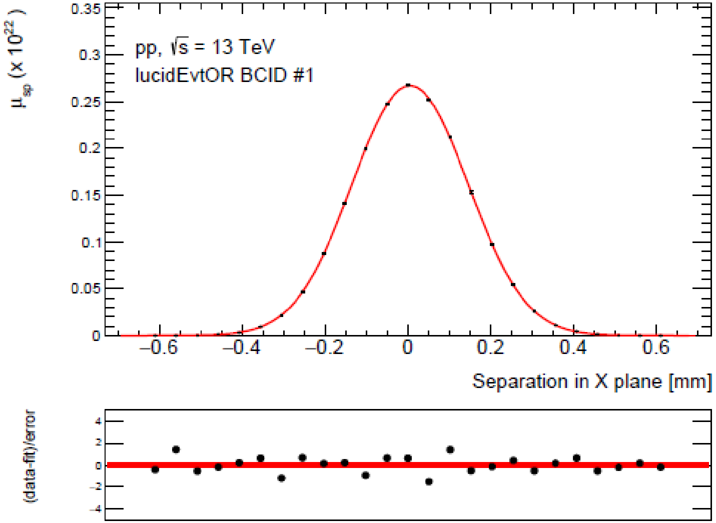

$$\int \rho_1(x)\rho_2(x)dx = \frac{\text{Rate}(\Delta=0)}{\int \text{Rate}(\Delta)d\Delta}$$

Luminosity and visible inelastic rate

$$\mathcal{L} = \frac{\mu_{\text{inel}}}{\sigma_{\text{inel}}} = \frac{\epsilon\mu_{\text{inel}}}{\epsilon\sigma_{\text{inel}}} \equiv \frac{\mu_{\text{vis}}}{\sigma_{\text{vis}}}$$

Luminometers

ATLAS uses several luminosity detectors:

- LUCID (Cherenkov detector)
  17 m away from interaction point
- BCM (Diamond detector)
  1.8 m away from interaction
- Inner detector (pixels, tracks, vertices)
- Calorimeters (current drawn)

Deduce visible inelastic rate from events failing OR selection, assuming Poisson statistics:

$$P(0) = e^{-\mu_{vis}}$$

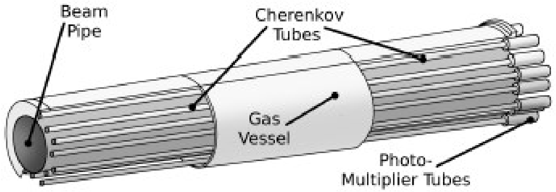

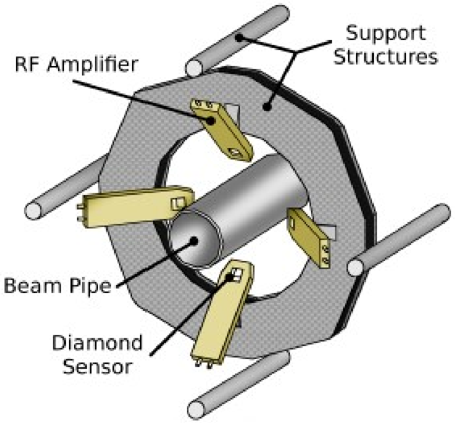

Fig from [6]

Absolute calibration with vdM method

$$\mathcal{L} = \frac{\mu_{\rm inel}}{\sigma_{\rm inel}} = \frac{\epsilon\mu_{\rm inel}}{\epsilon\sigma_{\rm inel}} \equiv \frac{\mu_{\rm vis}}{\sigma_{\rm vis}}$$

In dedicated runs: measure simultaneously $\mathcal{L}$ from machine parameters (vdM method) and visible rate, $\mu_{\rm vis}$ for a given detector, to get the constant $\sigma_{\rm vis}$

In normal runs: measure $\mu_{\rm vis}$ and divide by $\sigma_{\rm vis}$ to get $\mathcal{L}$

Beam-drift during vdM scans

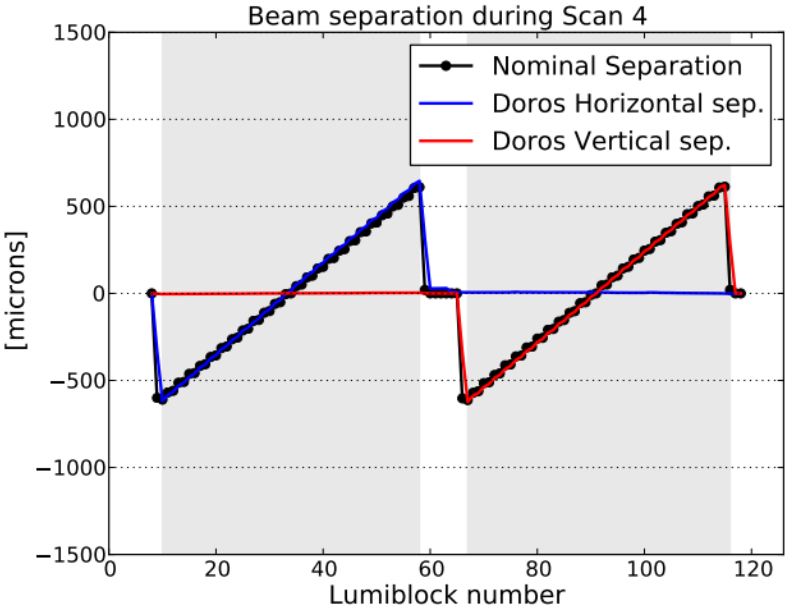

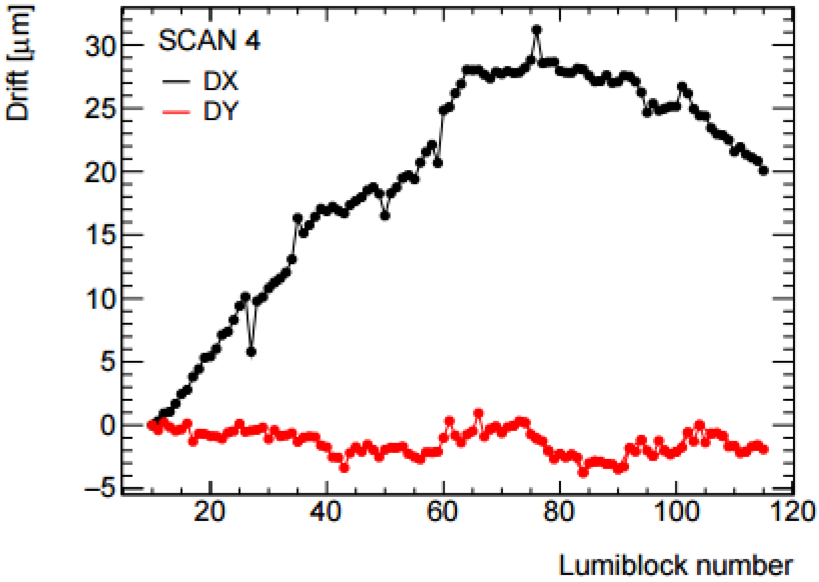

Corrections due to drift up to 2.4%

New instrumentation allows us to push down uncertainty to permil level

Scan-to-scan reproducibility

- We did have 3 different scans. The calibration constant should be the same in all of them

- Beam-drift reduces tension among scans, bringing down reproducibility uncertainty to ~0.6%

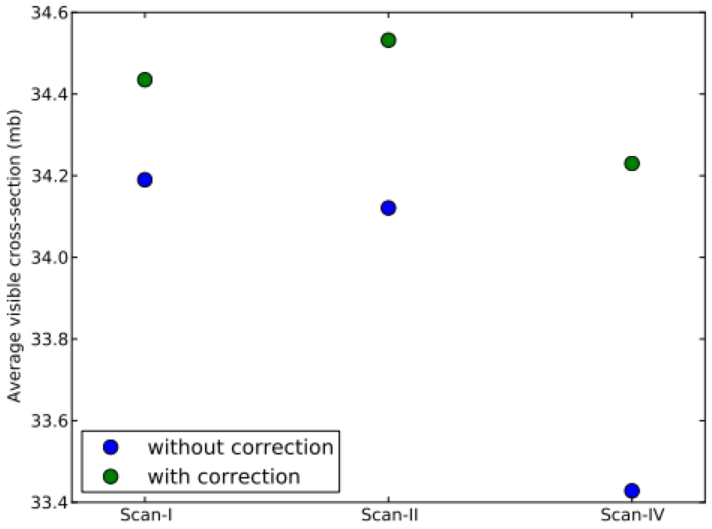

Beam-beam deflections

- Beams repel each other electromagnetically. Deflection can be calculated analytically
- It has the effect to distort the scan-curves leading to ~2% changes in calibration
- For the first time we have spotted beam-beam effects in beam-drift data. And it is consistent with expectations

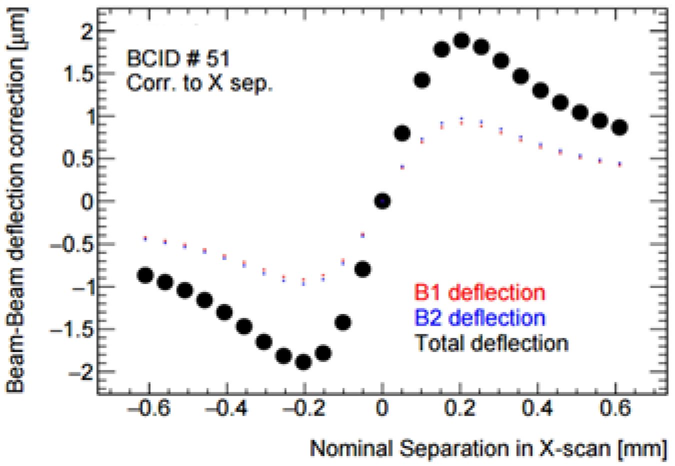

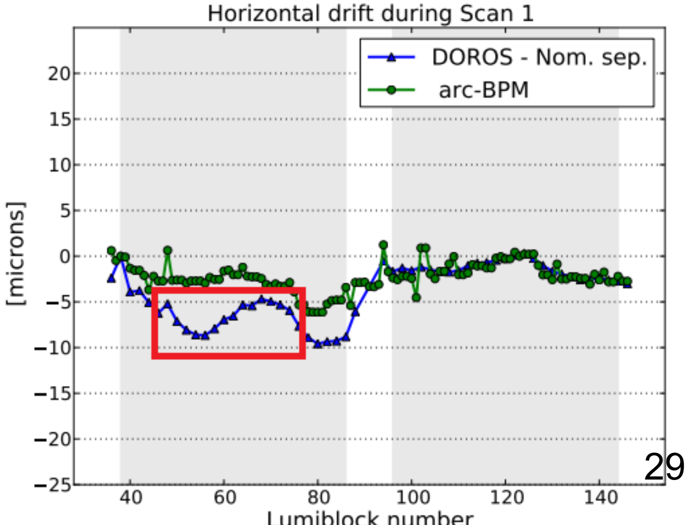

Non-factorization bias

Traditional vdM analysis assumes $$\rho(x,y) = \rho_x(x)\rho_y(y)$$

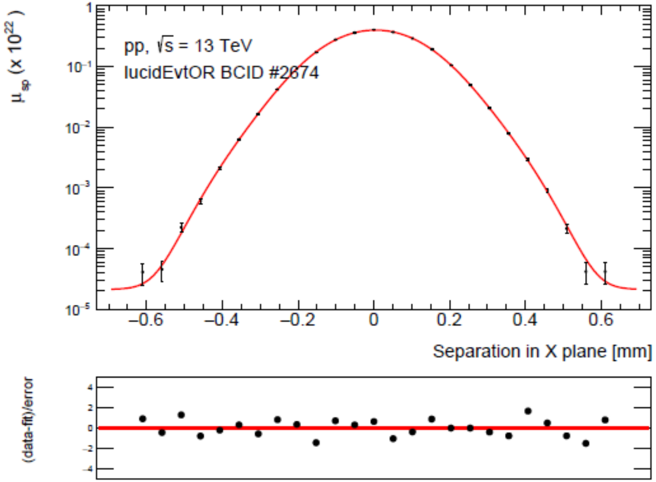

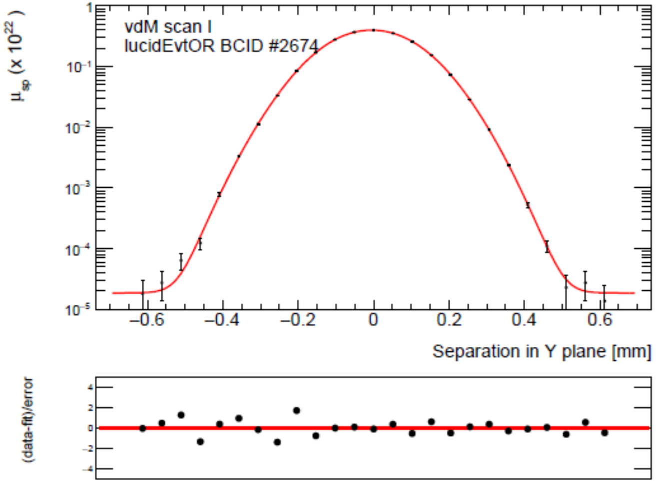

But it can be generalized, with simultaneous fit with “non-factorizable” function

~1% uncertainty

$$f(x,y) = e^{\frac{-x^2}{2\sigma_x^2}} e^{\frac{-y^2}{2\sigma_y^2}} [1 + pol(x) + pol(y)]$$

Luminosity uncertainty timeline

- EPS 2015 : 9.0 %
- End of year 2015 : 5.0 %
- **Today : 1.9 %**

Improvement largely due and beam-beam corrections, and understanding of non-factorization bias.

Constraining the fraction of diffractive events

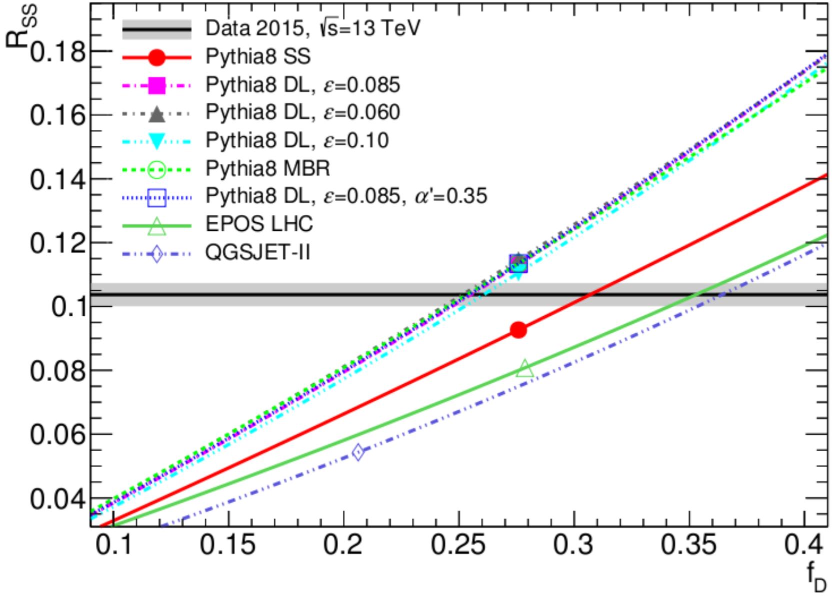

- Ratio of single-sided to inclusive events depends depends on

$$f_D \equiv \frac{\sigma_{SD}+\sigma_{DD}}{\sigma_{inel}}$$

- For each MC model, we tune f_D to match the data

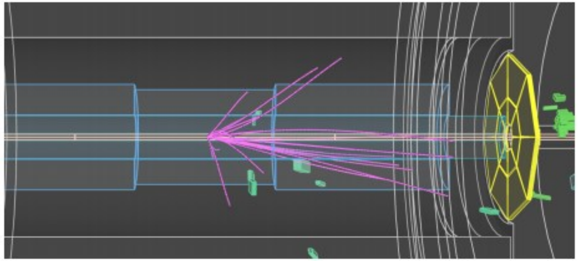

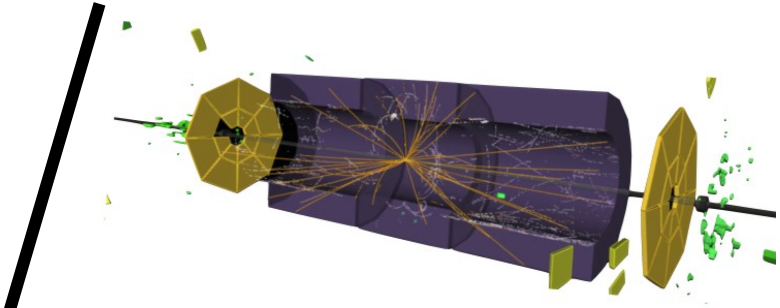

Inclusive hit distribution

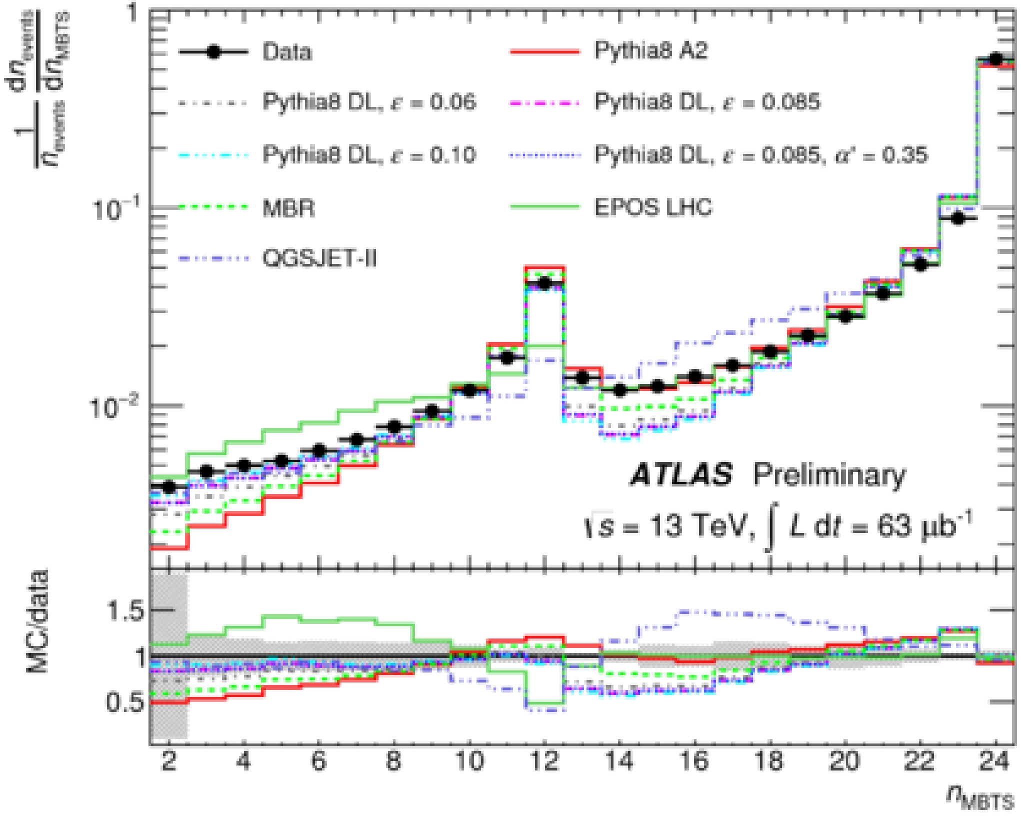

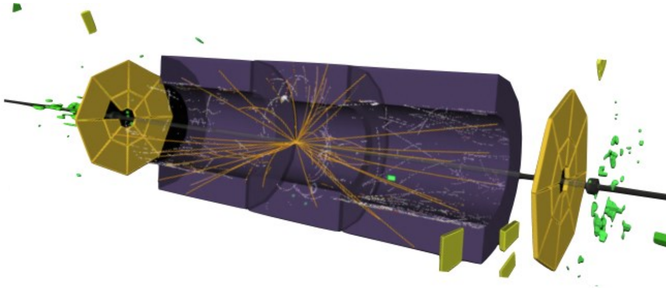

- Most of events fire every MBTS counter
- No MC model is perfect but some do better than others

Single-sided hit distribution

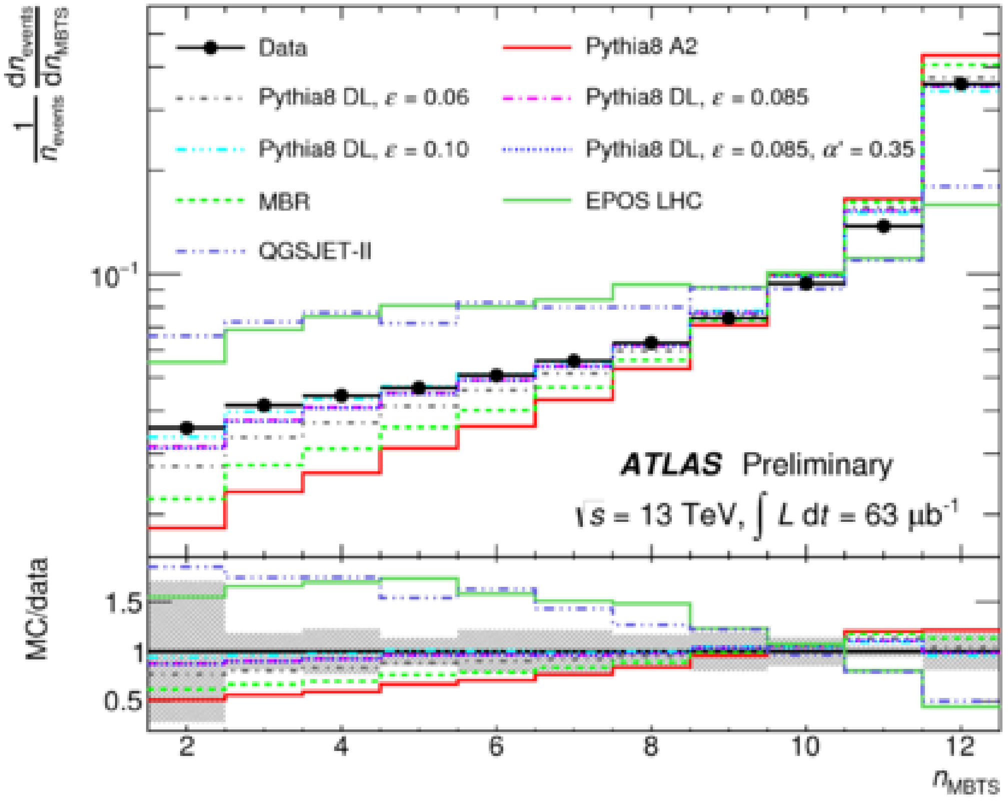

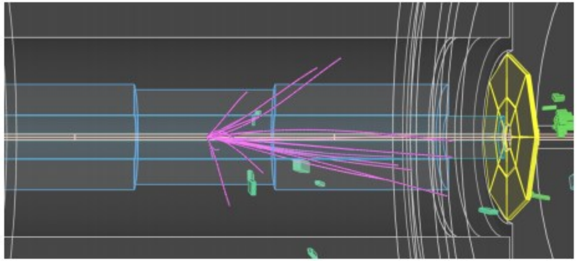

- Most of events contain high multiplicity
- Pythia DL models do a pretty good job.
- I.e, diffractive events within acceptance are reasonable well modelled.

Fiducial cross-section

$$\sigma(\tilde{\xi} > 10^{-6}) = \frac{(N - N_{\mathrm{BG}})}{\epsilon_{\mathrm{trig}} \times \mathcal{L}} \times \frac{1 - f_{\tilde{\xi}<10^{-6}}}{\epsilon_{\mathrm{sel}}}$$

Factor	Value	Rel. unc.
Number of selected events (N)	4159074	–
Number of background events (N_{BG})	43512	$\pm 100\,\%$
Luminosity [μb^{-1}] (L)	62.9	$\pm 9\,\%$
Trigger efficiency (ϵ_{trig})	99.7%	$\pm 0.1\,\%$
MC Correction factor ($(1 - f_{\tilde{\xi}<10^{-6}})/\epsilon_{\mathrm{sel}}$)	0.993	$\pm 0.5\,\%$

$$\sigma(\tilde{\xi} > 10^{-6}) = 65.2 \pm 0.8\ (\mathrm{exp.})\ \pm 5.9\ (\mathrm{lum.})\ \mathrm{mb}$$

Fiducial cross-section

$$\sigma(\tilde{\xi} > 10^{-6}) = 65.2 \pm 0.8\ (\text{exp.})\ \pm 5.9\ (\text{lum.})\ \text{mb}$$

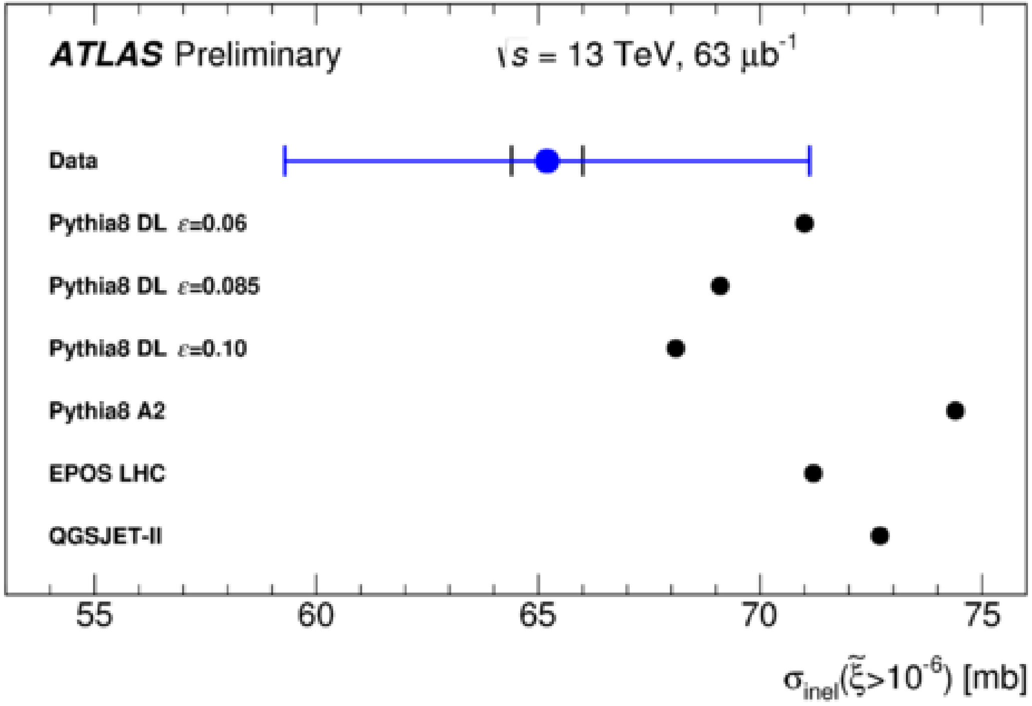

Total inelastic cross-section

To report total cross-section we need to correct for limited acceptance

$$\sigma(\tilde{\xi} > m_p^2/s) \quad = \quad \sigma(\tilde{\xi} > 10^{-6}) + \sigma(m_p^2/s < \tilde{\xi} < 10^{-6})$$

Measured

?

Total cross-section

$$\sigma(\tilde{\xi} > m_p^2/s) = 73.1 \pm 0.9 \text{ (exp.)} \pm 6.6 \text{ (lum.)} \pm 3.8 \text{ (extr.) mb}$$

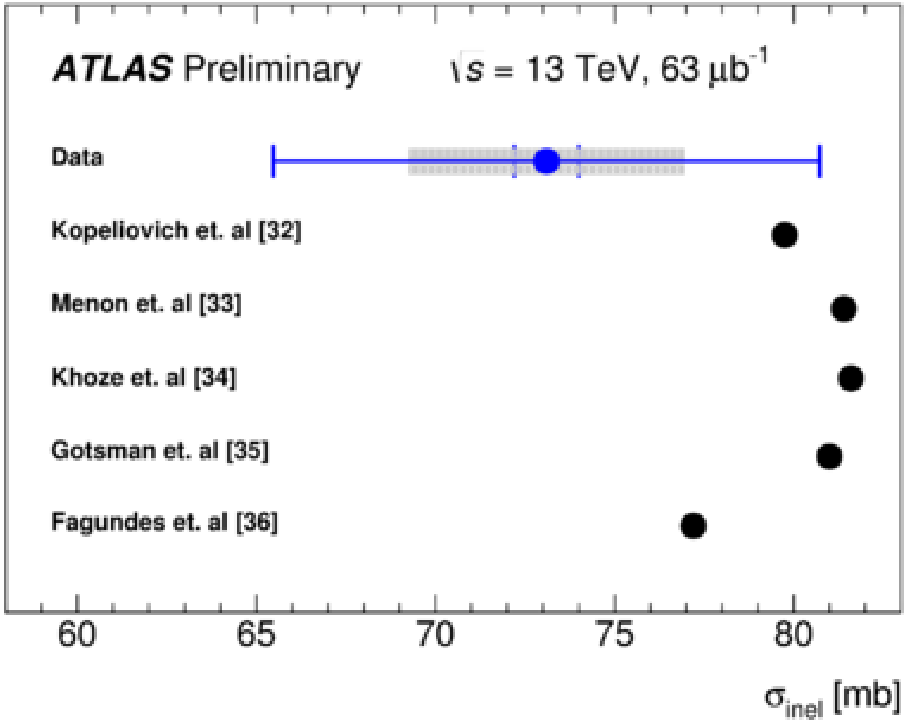

Total cross-section

$$\sigma(\tilde{\xi} > m_p^2/s) = 73.1 \pm 0.9\ (\text{exp.})\ \pm 6.6\ (\text{lum.})\ \pm 3.8\ (\text{extr.})\ \text{mb}$$

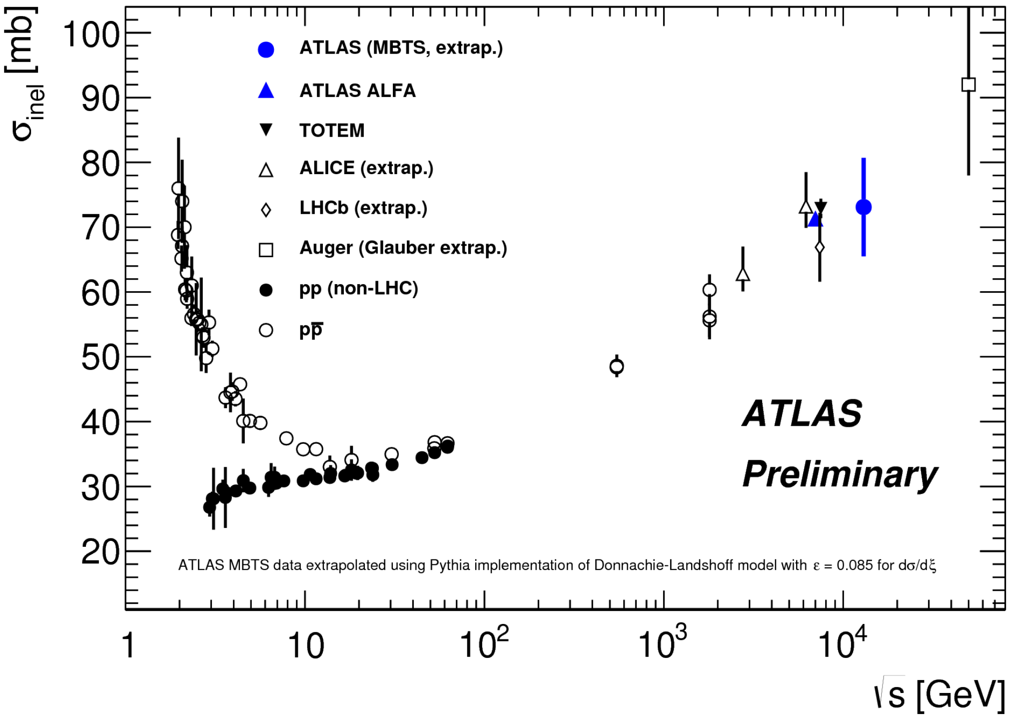

Constraining extrapolation with 7 TeV data

- ALFA result used elastic scattering and optical theorem to infer total inelastic cross-section
- MBTS result measured fiducial inelastic cross-section for $\tilde{\xi} > 5 \times 10^{-6}$

$$\begin{aligned}
\sigma_7(\tilde{\xi} < 5 \times 10^{-6}) &= \sigma_7(\tilde{\xi} > m_p^2/s) - \sigma_7(\tilde{\xi} > 5 \times 10^{-6}) \\
&= \sigma_{\mathrm{ALFA}} - \sigma_{\mathrm{MBTS}} \\
&= (71.34 \pm 0.91)\ \mathrm{mb} - (60.33 \pm 2.10)\ \mathrm{mb} \\
&= 11.01 \pm 2.29\ \mathrm{mb}
\end{aligned}$$

Extrapolation to total cross-section

$$\sigma_{13}(\tilde{\xi} > m_p^2/s) \;=\; \sigma_{13}(\tilde{\xi} > 10^{-6}) + \sigma_7(\tilde{\xi} < 5\times 10^{-6}) \times \frac{\sigma_{13}^{MC}(\tilde{\xi} < 10^{-6})}{\sigma_7^{MC}(\tilde{\xi} < 5\times 10^{-6})}$$

Measured

MC

1.015 ± 0.100

Source	$\frac{\sigma_{13}^{MC}(\tilde{\xi}<10^{-6})}{\sigma_7^{MC}(\tilde{\xi}<5\times10^{-6})}$
Pythia8 SS	0.782
Pythia8 DL $\epsilon = 0.085$	1.015
Pythia8 DL $\epsilon = 0.06$	1.04
Pythia8 DL $\epsilon = 0.10$	0.999
EPOS	1.051
QGSJET	1.093

76.3 mb = 65.2 mb + 11.1 mb

Result consistent with MC-based extrapolation, work in progress

Conclusions

- First measurement of inelastic cross-section at 13 TeV
- Preliminary result uncertainty dominated by luminosity (9%)
- Well controlled luminosity calibration and extrapolation uncertainties will add up to 3--4% (my educated guess, work in progress)

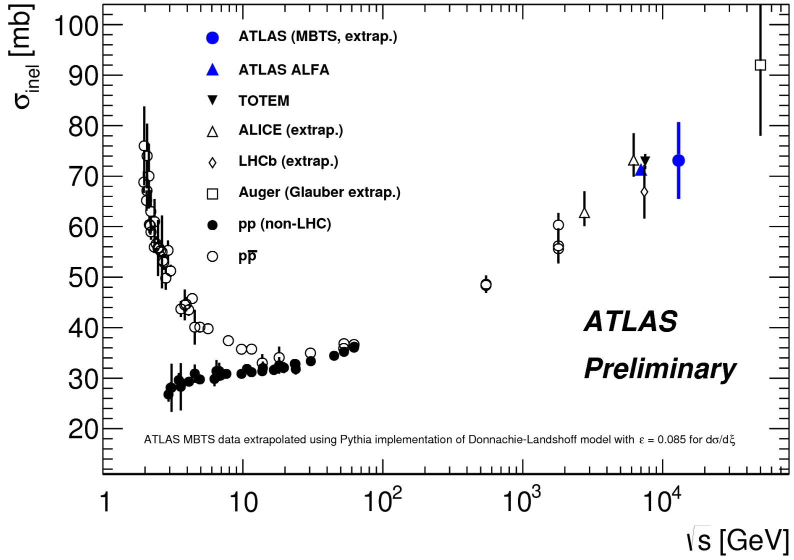

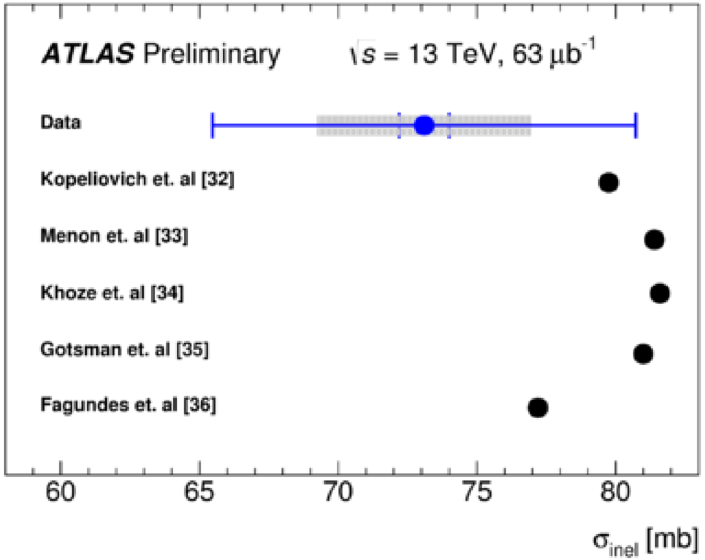

Back up slides

Acceptance

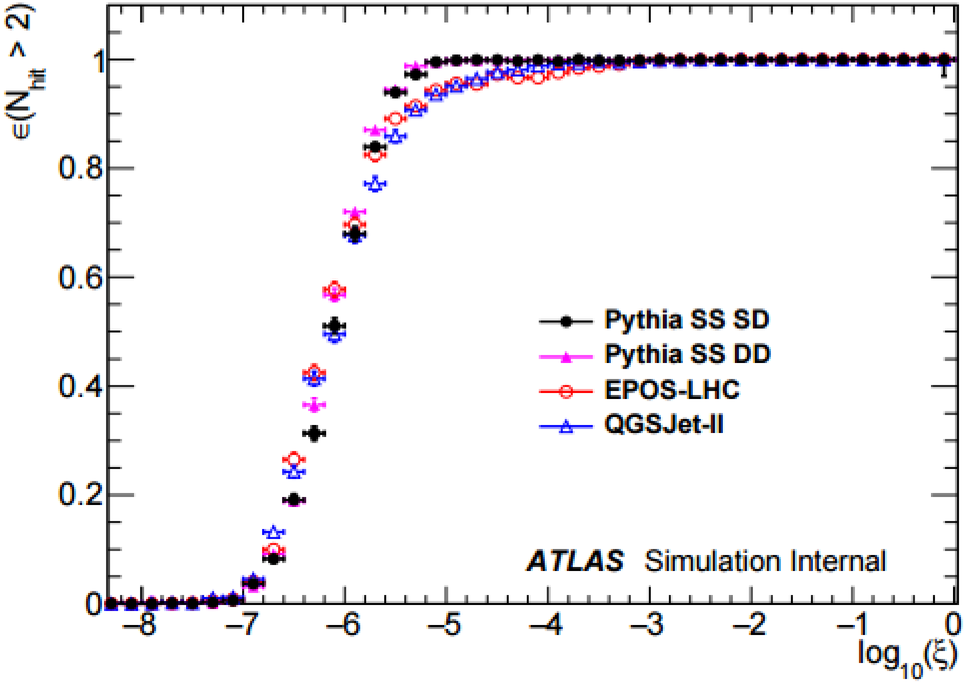

ε(N_hit > 2)
1
0.8
0.6
0.4
0.2
0
−8
−7
−6
−5
−4
−3
−2
−1
0
log10(ξ)
Pythia SS SD
Pythia SS DD
EPOS-LHC
QGSJet-II
ATLAS Simulation Internal

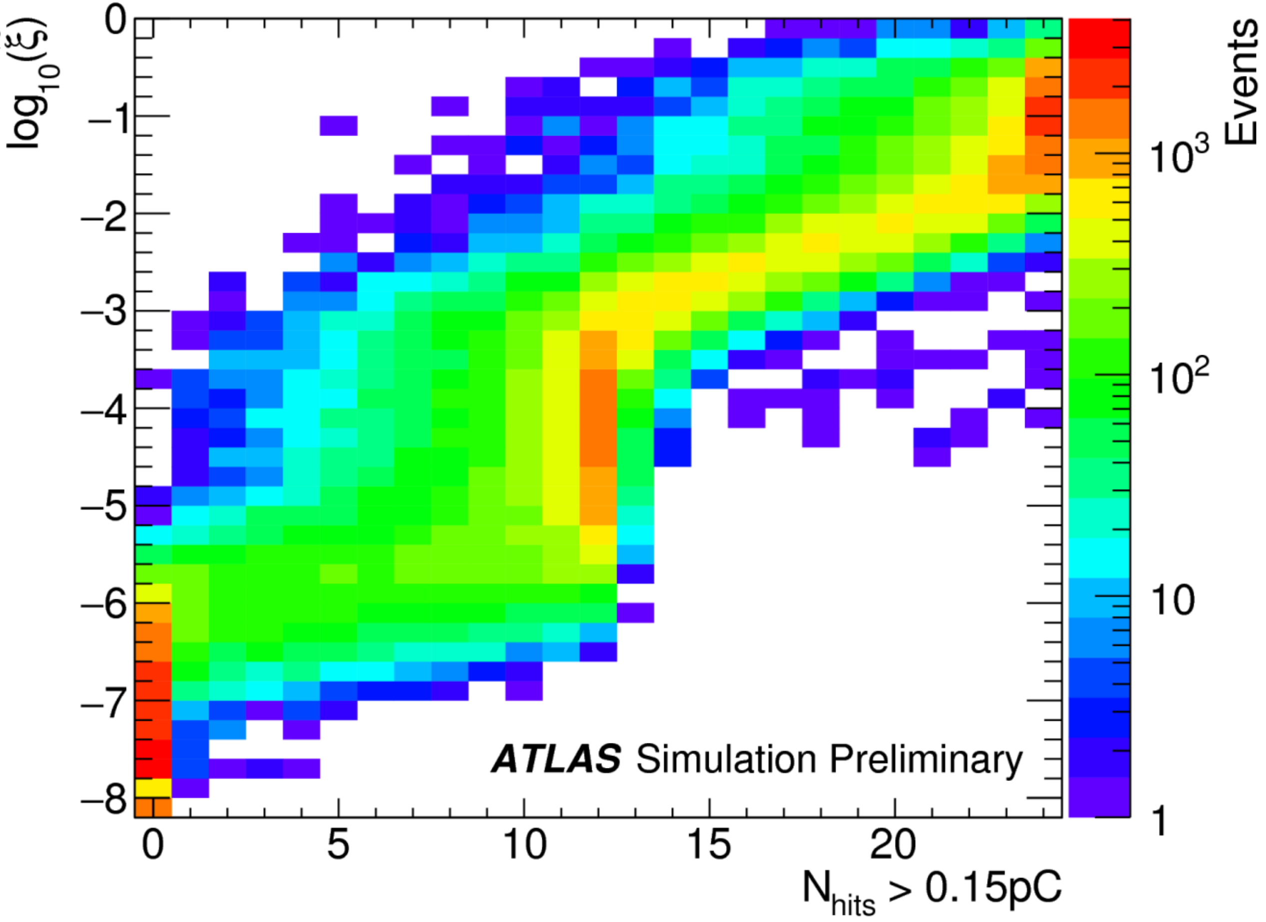

$\log_{10}(\tilde{\xi})$
0
−1
−2
−3
−4
−5
−6
−7
−8
0
5
10
15
20
N_{hits} > 0.15pC
Events
10^3
10^2
10
1
ATLAS Simulation Preliminary

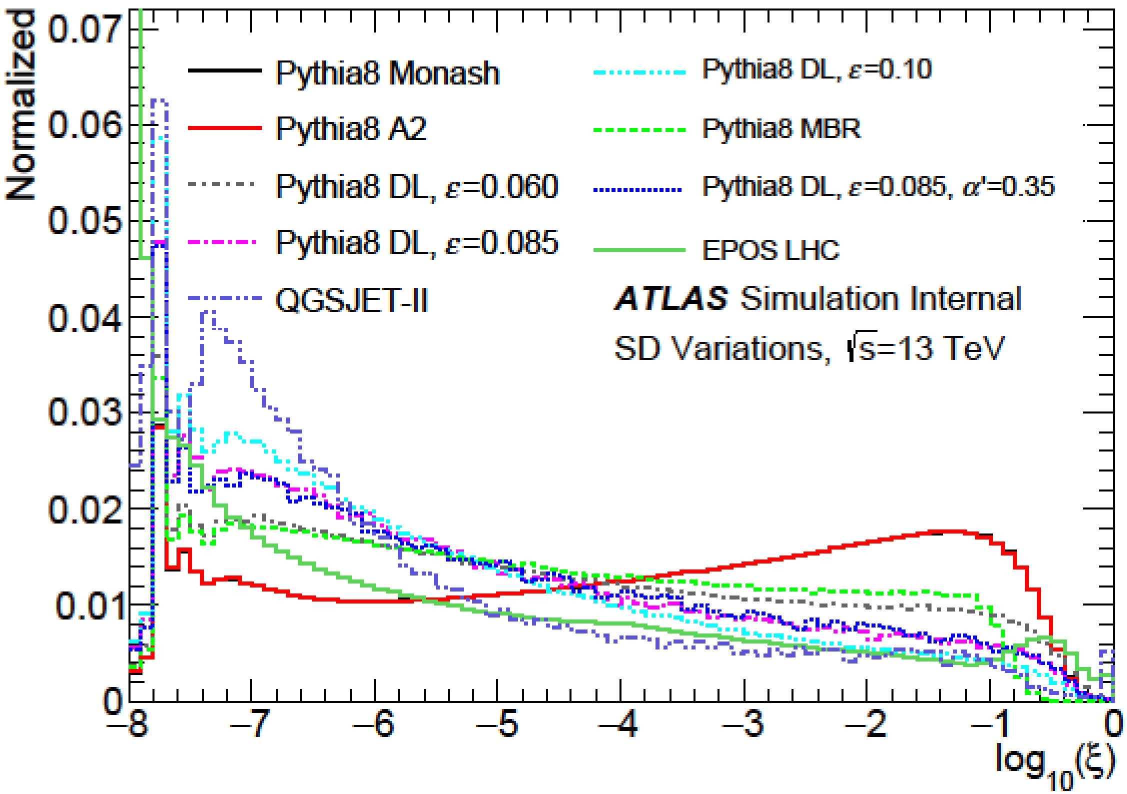

Normalized
0.07
0.06
0.05
0.04
0.03
0.02
0.01
0
−8
−7
−6
−5
−4
−3
−2
−1
0
log10(ξ)
Pythia8 Monash
Pythia8 A2
Pythia8 DL, ε=0.060
Pythia8 DL, ε=0.085
QGSJET-II
Pythia8 DL, ε=0.10
Pythia8 MBR
Pythia8 DL, ε=0.085, α'=0.35
EPOS LHC
ATLAS Simulation Internal
SD Variations, √s=13 TeV

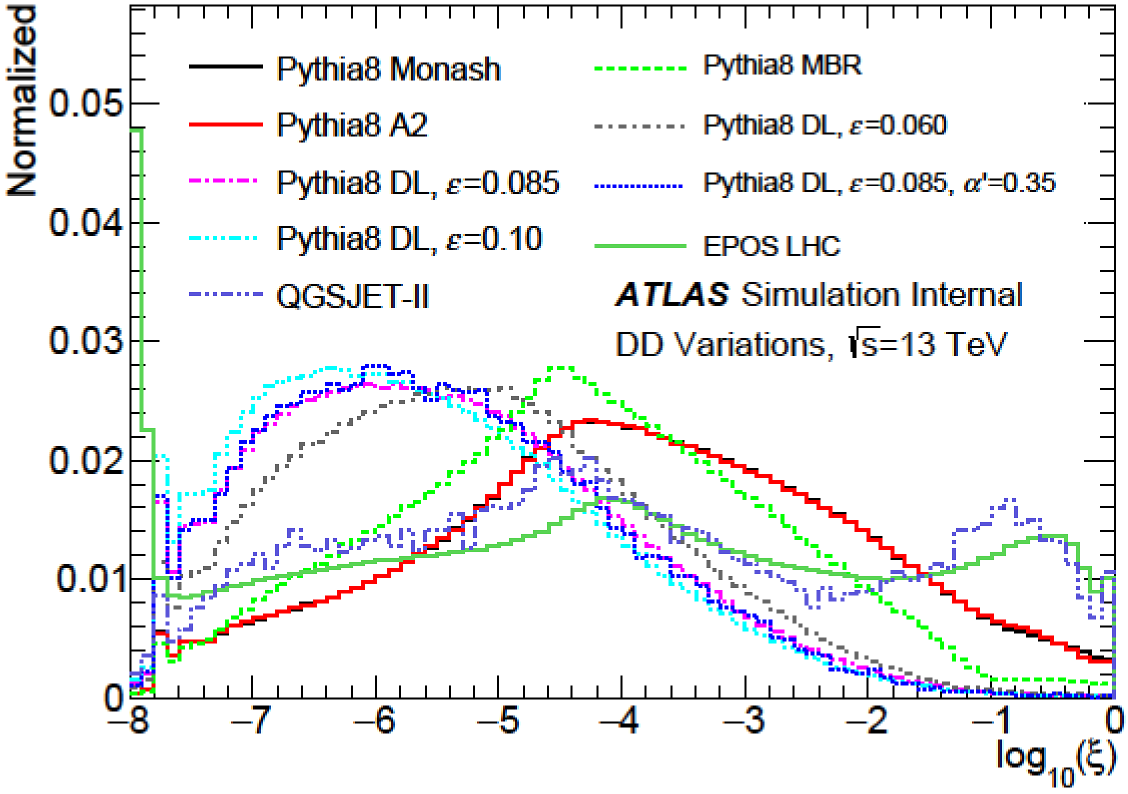

Normalized
0.05
0.04
0.03
0.02
0.01
0
−8
−7
−6
−5
−4
−3
−2
−1
0
log10(ξ)
Pythia8 Monash
Pythia8 A2
Pythia8 DL, ε=0.085
Pythia8 DL, ε=0.10
QGSJET-II
Pythia8 MBR
Pythia8 DL, ε=0.060
Pythia8 DL, ε=0.085, α'=0.35
EPOS LHC
ATLAS Simulation Internal
DD Variations, √s=13 TeV